Princeton Plasma Physics Laboratory

PPPL- 4571

PPPL- 4571

Stellarator Coil Design and Plasma Sensitivity

Long-Poe Ku and Allen H. Boozer

November, 2010

PPPL
PRINCETON PLASMA
PHYSICS LABORATORY

Prepared for the U.S. Department of Energy under Contract DE-AC02-09CH11466.

Princeton Plasma Physics Laboratory
Report Disclaimers

Full Legal Disclaimer

Trademark Disclaimer

PPPL Report Availability

Princeton Plasma Physics Laboratory:

http://www.pppl.gov/techreports.cfm

Office of Scientific and Technical Information (OSTI):

http://www.osti.gov/bridge

Related Links:

U.S. Department of Energy

Office of Scientific and Technical Information

Fusion Links

Stellarator coil design and plasma sensitivity

Long-Poe Ku
Princeton Plasma Physics Laboratory, Princeton University, Princeton, NJ 08543, lpku@pppl.gov
Allen H. Boozer
Columbia University, New York, NY 10027, ahb17@columbia.edu
(Dated: October 27, 2010)

The rich information contained in the plasma response to external magnetic perturbations can be used to help design stellarator coils more effectively. We demonstrate the feasibility by first developing a simple, direct method to study perturbations in stellarators that do not break stellarator symmetry and periodicity. The method applies a small perturbation to the plasma boundary and evaluates the resulting perturbed free-boundary equilibrium to build up a sensitivity matrix for the important physics attributes of the underlying configuration. Using this sensitivity information, design methods for better stellarator coils are then developed. The procedure and a proof-of-principle application are given that (1) determine the spatial distributions of external normal magnetic field at the location of the unperturbed plasma boundary to which the plasma properties are most sensitive, (2) determine the distributions of external normal magnetic field that can be produced most efficiently by distant coils, (3) choose the ratios of the magnitudes of the the efficiently produced magnetic distributions so the sensitive plasma properties can be controlled. Using these methods, sets of modular coils are found for the National Compact Stellarator Experiment (NCSX) that are either smoother or can be located much farther from the plasma boundary than those of the present design.

I. INTRODUCTION

If the pressure and the rotational transform (or the plasma current) are specified as functions of the toroidal magnetic flux and the shape of the outermost magnetic surface is given, a toroidal plasma equilibrium is defined [1]. The shape is frequently chosen to optimize plasma equilibria to be stable at high beta and to have neoclassical transport that is sufficiently small. Once a plasma shape is obtained that has favorable properties, coils must be found that produce the required external magnetic fields.

The coils that surround a toroidal plasma have two functions: (1) produce the toroidal magnetic flux and (2) produce external magnetic fields necessary to make the total field normal to the plasma surface zero. A given plasma equilibrium requires coils produce both a definite toroidal magnetic flux and a normal magnetic field on its outermost surface. Unfortunately, the properties of Laplace's equation, $\nabla^2\Phi = 0$, imply that practical coils cannot produce the normal magnetic field that results from a stellarator optimization [2].

Between the coils and the plasma the magnetic field produced by the coils has the form

$$\vec{B}_c = \frac{\mu_0 G_0 \hat{\phi}}{2\pi R} + \vec{\nabla}\Phi \qquad (1)$$

with $\nabla^2\Phi = 0$. The potential Φ is specified by $\vec{B}_c \cdot \hat{n} = (\mu_0 G_0/2\pi R)\hat{\phi} \cdot \hat{n} + \hat{n} \cdot \vec{\nabla}\Phi$ on the plasma surface. The magnitude of $\vec{B}_c$ increases exponentially away from the surface, and various spatial distributons of $\vec{B}_c \cdot \hat{n}$ on the plasma surface for a given toroidal magnetic flux are associated with different rates of exponentiation. The normal magnetic field that the coils must supply to support an equilibrium produced by an optimization contains, in general, distributions that exponentiate too rapidly to be produced faithfully by coils.

The traditional method for dealing with the absence of consistency between optimized plasma shape and practical coils for supporting these shapes is to design coils at a practical distance from the plasma that minimize the root-mean-square (RMS) deviation of the normal magnetic field from zero on the desired plasma surface [3] [4]. A smaller RMS deviation implies more difficult coils, so a small enough RMS deviation is typically chosen such that an equilibrium obtained will adequately approximate the properties of the original optimized equilibrium. The traditional procedure for obtaining practical coils for an optimized stellarator equilibrium implicitly assumes that, by minimizing the RMS deviations, degradation of the optimized properties of the plasma will also be minimized, irrespective of the plasma sensitivity to the distributions of the deviations. This procedure would be optimal only if the plasma had the same sensitivity to all external magnetic perturbations, which it does not.

Alternatively, methods have been proposed to minimize the normal surface displacements from the desirable plasma shape, instead of minimizing the RMS deviations of the normal magnetic field from zero [5]. Such methods implicitly assume, also, that the plasma has the same sensitivity to all displacements. The procedures developed, thus, lead to similar coil solutions as those from the traditional method, which are not optimal. It is possible to optimize directly the properties of the plasma by varying the geometry of the coils [6]. But because of the vastness of the configuration space in stellarators, a 'good' initial coil geomerty is often needed to converge on finding the desirable final solution that matches the original optimized equilibrium. The initial geometry is typically

gotten from using the traditional procedure.

The study in this paper has two purposes: (1) to develop a method for finding the mode perturbations that degrade the physics properties the most and need to be carefully controlled for a stellarator plasma whose shape is known, (2) to demonstrate that information of the plasma response to magnetic field perturbations can be used to help design coils more efficiently.

In Ref.[7], it was shown that the standard δW method for the ananlysis of the ideal magnetohydrodynamic (MHD) stability also gives the response of a plasma to small perutrbations. In this paper, we present a direct approach for the study of the effects of magnetic perturbations. The method, which is essentially a numerical experiment, is to apply a small external magnetic field perturbation directly to the boundary of an otherwise stable, quasi-axisymmetric configuration and then observe how the plasma responds. The plasma, responding to the perturbation, will re-establish a state of equilibrium by altering the shape such that the magnetic fields normal to all plasma surfaces become zero. The current potential on a surface located at a small distance from the plasma is calculated such that the normal magnetic fields, including the perturbation, vanish on the plasma boundary. The free-boundary equilibrium supported by the magnetic fields from this current potential manifests the plasma response to the perturbation. In section II the algorithm for the boundary perturbation method is outlined. In section III the method is applied to NCSX to study the sensitivity of the plasma response to different modes of perturbations. Our method can be applied to non-symmetric, periodicity breaking perturbations by treating numerically a configuration as having one field period and using both even and odd functions to describe the stellarator geometry. For this paper, however, we consider only the perturbations that are stellarator symmetric and periodicity preserving. These are the perturbations important for coil designs.

Each favorable plasma property has a range of sensitivities to the distributions of external perturbations to the normal magnetic field on the plasma surface. This paper finds only the perturbation distributions to which the plasma has the greatest sensitivity and shows that the solutions for the coils can be simplified by minimizing the errors in these distributions rather than in just RMS normal field. The method can and should be extended to include additional distibutions of high plasma sensitivity. In section IV algorithms are discussed that use the plasma response to magnetic field perturbations to help design coils more efficiently. There are two methods developed: one is to use the sensitivity data to construct a basis for representing normal magnetic fields on the plasma boundary and the other is to use the sensitivity data to construct an importance vector to differentiate components in the normal magnetic fields that should carry more weight in the coil design. Taking advantage of the importance information, we have developed a new method for designing coils for stellarators. The new method uses the technique of singular value decomposition for the inductance matrix that relates the magnetic flux on the plasma surface to the current potential on the coil winding surface. A small set of singular values producing the magnetic field distributions that decay most slowly through space and can, therefore, be produced most efficiently by distant coils are retained. For each of the retained singular values a coil set is derived from the respective current potentials. The coil currents associated with these coils are then varied to find equilibria in the neighborhood of the target plasma which have similar physics properties as those of the originally optimized plasma. We apply this method to find a new set of modular coils for NCSX at a plasma-coil separation far greater than the present design (0.21 units of the major radius versus 0.14 units). Coils at this separation would otherwise be extremely difficult to find.

In section V we give a summary and outline possible future studies.

II. ALGORITHM FOR THE BOUNDARY PERTURBATION METHOD

The normal component of magnetic fields on the last closed magnetic surface (LCMS), $\vec{b}\cdot\hat{n}$, may be expanded with respect to a basis set:

$$\vec{b}\cdot\hat{n} = \sum_{m,n} w\Phi_{m,n} f_{m,n}(\theta,\phi) \tag{2}$$

where m and n are poloidal and toroidal mode numbers, θ and ϕ are poloidal and toroidal angles, w is an arbitrary weight and $f_{m,n}$ are orthonormal functions satisfying

$$\int w f_{m,n} f_{m',n'} da = \delta_{mm',nn'} \tag{3}$$

Here, da is the area element and $\delta_{mm',nn'}$ is the Kronecker delta. According to Maxwell's equations, all sources of magnetic fields outside the plasma may be represented by current densities associated with a scalar potential function κ on an arbitrary chosen surface [3],

$$J = \nabla\kappa \times \hat{n} \tag{4}$$

The current potential, κ may be similarly expanded with respect to a basis set $g_{m,n}(\theta,\phi)$,

$$\kappa = \sum_{m,n} I_{m,n} g_{m,n}(\theta,\phi) \tag{5}$$

For a given LCMS geometry and the geometry of the current carrying surface, a mutual inductance matrix $[M]$ which relates the current potential on the current carrying surface to the normal fields on LCMS may be constructed using the Biot-Savart law

$$\vec{b}\cdot\hat{n} = (\nabla\times\vec{A})\cdot\hat{n} \tag{6}$$

$$\vec{A}(\vec{x}) = \frac{\mu_0}{4\pi}\int \frac{J(\vec{x}')}{\mid \vec{x}-\vec{x}' \mid}\cdot da' \tag{7}$$

Here $\vec{x}$ and $\vec{x}'$are positions on the LCMS and on the current carrying surface, respectively. Introducing a magnetic field perturbation

$$\delta\vec{b}\cdot\hat{n} = \sum_{m,n} w\delta b_{m,n} f_{m,n}(\theta,\phi) \tag{8}$$

and a column vector, $[\vec{b}\cdot\hat{n}]_{plasma}$, for the normal field harmonics due to the plasma current on LCMS, the magnetic fields required to support the perturbed equilibrium can be obtained from κ , which satisfies

$$[M]\cdot[I] = -[\vec{b}\cdot\hat{n}]_{plasma} + [\delta b\cdot\hat{n}] \tag{9}$$

By varying the field perturbation mode by mode, solving the free-boundary equilibrium for the force balance and evaluating the properties of the resulting equilibrium, we obtain a sensitivity matrix, $[R]$, whose rows are changes in different types of physical response F and whose columns are perturbations of different modes:

$$[R]\cdot[\delta\vec{b}\cdot\hat{n}/\mid\vec{b}\mid] = [\delta F/F] \tag{10}$$

Despite the simplicity of the concept and the straightforwardness of the method, we need to be very careful doing calculations at every step in practice in order to distinguish numerical errors from the true effects of small perturbations. A code, BNPERT, has been written for this purpose which uses parallel multi-processing to efficiently evaluate plasma responses to perturbations of different modes. The equilibrium is obtained using VMEC [8] in the present version. The current potential, κ, was calculated on a surface in a coordinate system defined by the normalized poloidal angle u and toroidal angles v ($u=\theta/2\pi$, $v=N_p\phi/2\pi$, N_p is the number of field periods and $0\le u,v<1$). The unit square was divided into 64 by 64 grid points. The normal magnetic fields were typically represented by a double Fourier series with 10 poloidal modes and 10 toroidal modes. For perturbations that preserve stellarator symmetry and periodicity the Fourier series takes on the form of sine functions. Perturbations in the external magnetic field were studied for the poloidal and toroidal modes m and n in the range of $0\le m\le 9$ and $-5\le n\le 5$. In calculating the magnetic fields needed by VMEC, the current potential was represented by 60 filamentary coils for each field period derived by dividing the plane of the normalized poloidal and toroidal angles into 256 by 256 meshes. The magnetic fields encompassing the plasma region were evaluated by the Biot-Savart law in 201 radial and 201 axial grid points on 32 toroidal planes for each field period. VMEC calculations were carried out typically with 11 poloidal modes and 8 toroidal modes and with 49 flux surfaces. Our experience indicates that linear responses may be studied for perturbations as small as $\sim 0.01\%$. In our evaluation of the plasma properties, we included the response of the external kink, ballooning, Mercier and resistive interchange modes, the effective helical ripples, plasma beta, aspect ratio, rotational transform, global magnetic shear, residues in the magnetic spectrum as well as the areas of secondary ripple wells along a chosen field line segment. In the analysis of plasma stability to the kink modes for stellarators having field periods N_p, Fourier harmonics due to perturbations with a toroidal mode number n are coupled to $n+kN_p$ (k an integer). As a result, there are $N_p/2$+1 families of mode perturbations for even N_p and (N_p-1)/2+1 families for odd N_p. In particular, for N_p=3 there are two families of mode perturbations, N=0 and N=1, and we have included them both in the study of the plasma response in the next section. Using the magnetic coordinates the width of magnetic island caused by the perturbation on a mode rational surface corresponding to the rotational transform, $\iota = n/m$, in units of toroidal flux enclosed by the plasma, was assessed by

$$\delta s = 4\cdot\sqrt{(\frac{\vec{b}\cdot\nabla s}{\vec{b}\cdot\nabla\phi})_{m,n}\cdot\frac{1}{m\iota'}} \tag{11}$$

where s is the normalized toroidal flux labelling the surfaces, ϕ is the toroidal angle and the prime denotes the derivative with respect to s. The normal component of the magnetic field in the evaluation was calculated using filamentary coils to represent the perturbed current potential. It does not include the resistive effects or effects due to the plasma pressure and current. Using PIES code [9] to make a more complete assessment of islands caused by magnetic perturbations remains a possibility but the computational time is prohibitive with the present version of the code.

For the kink mode, the response was evaluated using TERPSICHORE [10]. Because configurations of interest are normally near marginal stability, the plasma response may not be linear even though the perturbation is small. To ensure the linearity in response we included an extra driving factor for the current and pressure, typically $\sim 3-5\%$, to destabilize plasmas just away from the marginal stability. The ballooning modes were evaluated using COBRA [11] on two field lines approximately passing through the outboard mid-plane at toroidal angles corresponding to the beginning of a field period and at the half period. The total area under which the modes were unstable was calculated and used as a metric. The Mercier and resistive interchange were evaluated by JMC [12]. Helical ripples were calculated by NEO [13] at five surfaces at radii corresponding to 10, 30, 50, 70 and 90% of the normalized toroidal flux. On each surface, the poloidal and toroidal angles were divided into 512 by

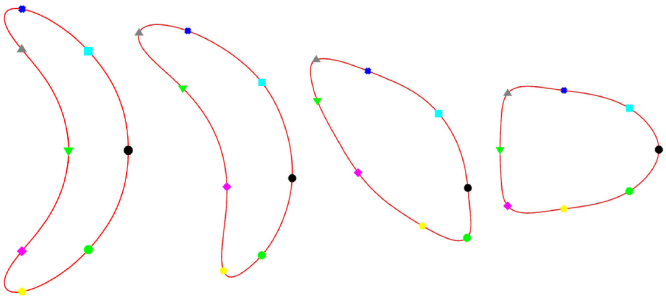

FIG. 1: (Color online) Four cross sections of NCSX at 4%β in equally spaced toroidal angles over half period. The four cross sections correspond to the normalized toroidal angles $v = N_p\phi/2\pi = 0.0$, 0.17, 0.33 and 0.5, respectively. For each cross section, the normalized poloidal angles $u = \theta/2\pi$ are shown in equal increment of 0.125 starting from $u = 0$ as a filled black circle and going counter-clockwise. The machine axis is to the left.

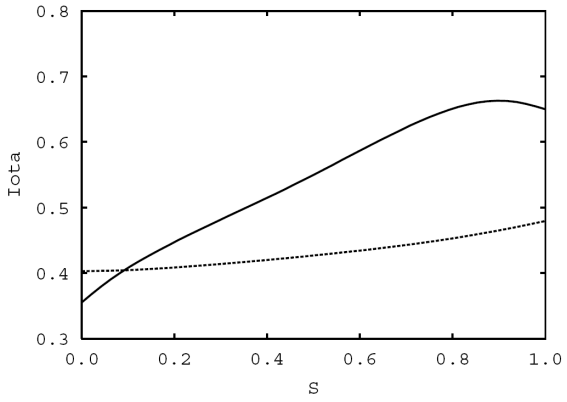

FIG. 2: (Color online) The rotational transform of NCSX as function of normalized toroidal flux s ($\sim r^2/a^2$). The dotted line is the rotational transform due to plasma shaping; the solid line is the toal transform including the contribution from plasma current at 4% β.

512 grids and the equilibrium was mapped to the Boozer magnetic coordinates [14] with the number of the poloidal modes chosen to be six times the number of modes used in VMEC and the number of the toroidal modes twice as many. There were 512 test particles with 512 steps used in the field line integration for each field period and at least 2048 periods were used in the integration in NEO calculations. Finally, the rotational transform calculated by VMEC was linearly interpolated to identify rational surfaces.

The linearity of plasma response can be checked by simply reversing the sign of a perturbation. However, the method is not restricted to just small linear perturbations. In addition, the perturbation can be periodicity-breaking or in violation of the stellarator symmetry, but both sine and cosine functions have to be used for the complete magnetic field representation and calculations become much more time-consuming.

III. EFFECTS OF MAGNETIC FIELD PERTURBATIONS IN NCSX

In this section, we present results from a study in which magnetic field perturbations were introduced to the reference NCSX plasma [15]. The general characteristics of the unperturbed NCSX are summarized in figure 1: the four cross sections of the plasma equally spaced in half-period, and in figure 2: the rotational transform. The configuration has three field periods and has an aspect ratio 4.5. It is stable to the external kink modes and is nearly stable to the ballooning modes at 4% β according to the ideal, linear MHD analysis. The configuration is quasi-axisymmetric and the magnitudes of effective helical ripples are generally $\leq 1\%$.

The sensitivity of the N=1 kink stability to different modes of perturbation, one Fourier mode at a time, is shown in figure 3. The sensitivity of the island width, excluding the plasma response, on the mode rational surface corresponding to $m = 5, n = 1$ is given in figure 4. The significance of the mode perturbation is clearly seen for those corresponding to the rational values (and the side bands) in the rotational transform. Similar characteristic is observed for the sensitivity of the ballooning stability as illustrated in figure 5. NCSX was specifically optimized for the kink stability by adjusting the boundary geometry. The optimization process brought the configuration to the boundary of marginal stability so that it is very sensitive to certain perturbations in the external magnetic fields. The evaluation of the plasma response has implicitly assumed the existence of nested flux surfaces in the entire plasma volume. At mode rational surfaces, parallel currents will develop under this assumption to prevent the opening of magnetic islands. The magnetic field perturbations in resonance with these rational modes tend to result in the local amplification with significant effects.

In figure 6 we show the sensitivity of the effective helical ripple on the flux surface at $r/a \sim 0.7$. The response spectrum is broad and the important effects tend to be from lower order modes. The sensitivity characteristic is clearly different from that for the MHD stability. Finally, in figure 7 we show the sensitivity of the aspect ratio to illustrate yet another different characteristic of the mode sensitivity. For the aspect ratio (and also the beta), the singularly most important mode of perturbation is the axisymmetric $m = 1$ and $n = 0$ mode, but the sensitivity is much weaker compared to that for the MHD stability.

The response matrix $[R]$ may be decomposed, using the method of singular value decomposition (SVD), into two 'input' and 'output' matrices, $[V]$ and $[U]$, and a matrix $[W]$ containing singular values, i.e.,

$$[R] = [U] \cdot [W] \cdot [V]^T \tag{12}$$

Column vectors in $[V]$ and $[U]$ are orthonormal. Perturbation distributions corresponding to large singular val-

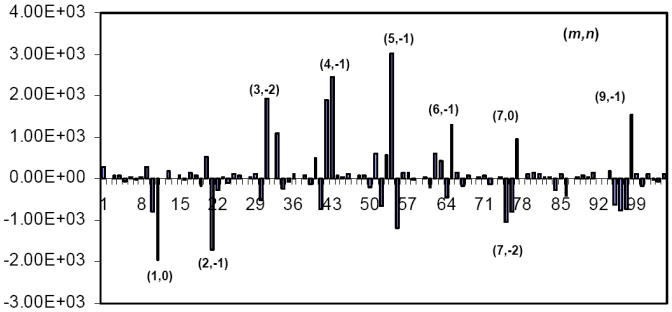

FIG. 3: (Color online) Sensitivity of the N=1 kink mode to external field perturbation for NCSX. The perturbation is represented as a Fourier series $\sum_{m,n} \delta b_{mn} \cdot sin(mu + nv)$ in the normalized poloidal angle u and toroidal angle v. The abscissa is the perturbation mode sequence grouped in poloidal mode numbers $m = 0, 9$ and for each poloidal mode number grouped in toroidal mode numbers $n = -5, 5$ except for $m = 0$ where $n = 0, 5$. The ordinate is the sensitivity response defined as per unit change in response per unit change in the external field, $\delta F/F/\delta b_{mn}/ \mid \vec{b} \mid$. Here the unit change in response is the change in the N=1 kink eigenvalue. In arriving at the figure, each δb_{mn} on the plasma surface was perturbed independently one at a time and the resulting free-boundary equilibrium was evaluated. Modes of significant sensitivity are highlighted and shown in mode pair (m, n), where m is the poloidal mode number and n is the toroidal mode number. For definitions of u and v, see figure 1.

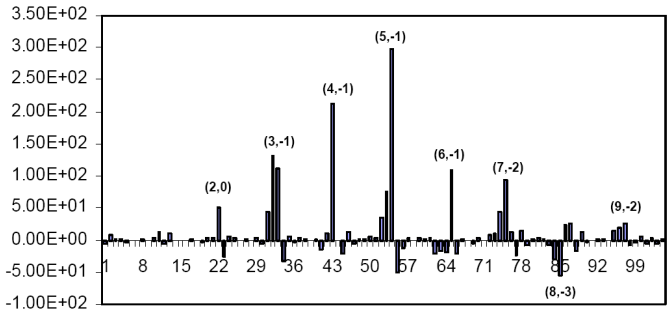

FIG. 4: (Color online) Sensitivity of the size of the magnetic island at the rational surface $\iota = 1/5$ to the external perturbation for NCSX. See figure 3 for details.

ues in $[W]$, which are respective column vectors of $[V]$, are the ones that the plasma is most sensitive to. The different types of response may also be combined into a total response function. Let $[\sigma]$ be a column vector containing weights given to various responses, such as those used to form the overall penalty function in arriving at the optimized configuration, then $[R]^T \cdot [\sigma]$ is a column vector containing the relative importance of each perturbation mode in $\delta\vec{b} \cdot \hat{n}$ on the plasma surface. The singular value decomposition of $[R]^T \cdot [\sigma]$ yields one non-zero singular value and the corresponding vector in the input matrix represents the perturbation distribution that the configuration is most sensitive to in its overall effect on

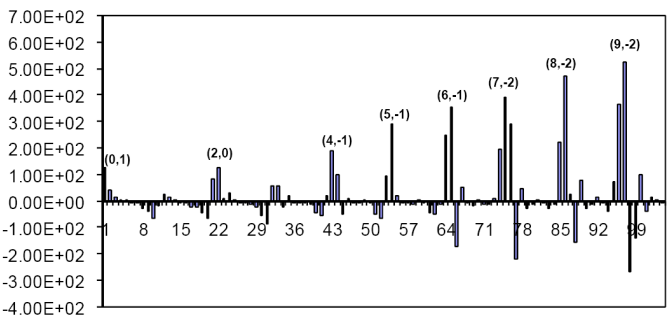

FIG. 5: (Color online) Sensitivity of the ballooning mode stability to the external perturbation for NCSX. See figure 3 for details. The high Fourier mode numbers in the sensitivity are associated with ballooning modes near the plasma edge.

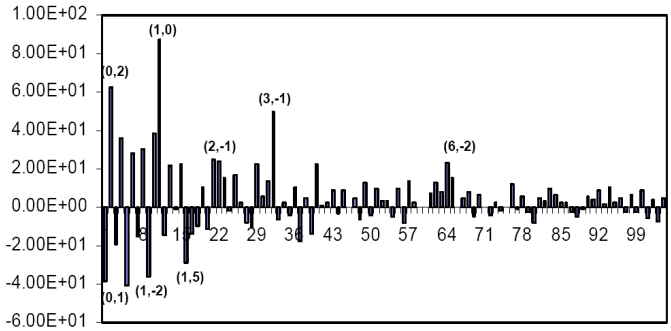

FIG. 6: (Color online) Sensitivity of the effective helical ripple to the external field perturbation at $r/a = 0.5$ for NCSX. See figure 3 for details.

the quality of the configuration.

In practice, however, it is more instructive to examine the characteristics of perturbation distributions separately for the important physics attributes of a configuration of interest. In figures 8 and 9 we show, for NCSX, the distributions of magnetic perturbations to which the N=1 external kink mode and the effective helical ripple at $r/a \sim 0.7$ are most sensitive. The two distributions are nearly orthogonal. It is interesting to note that for

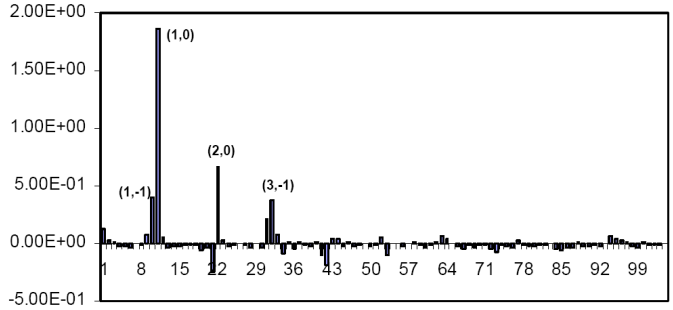

FIG. 7: (Color online) Sensitivity of the plasma aspect ratio to the external field perturbation for NCSX. See figure 3 for details.

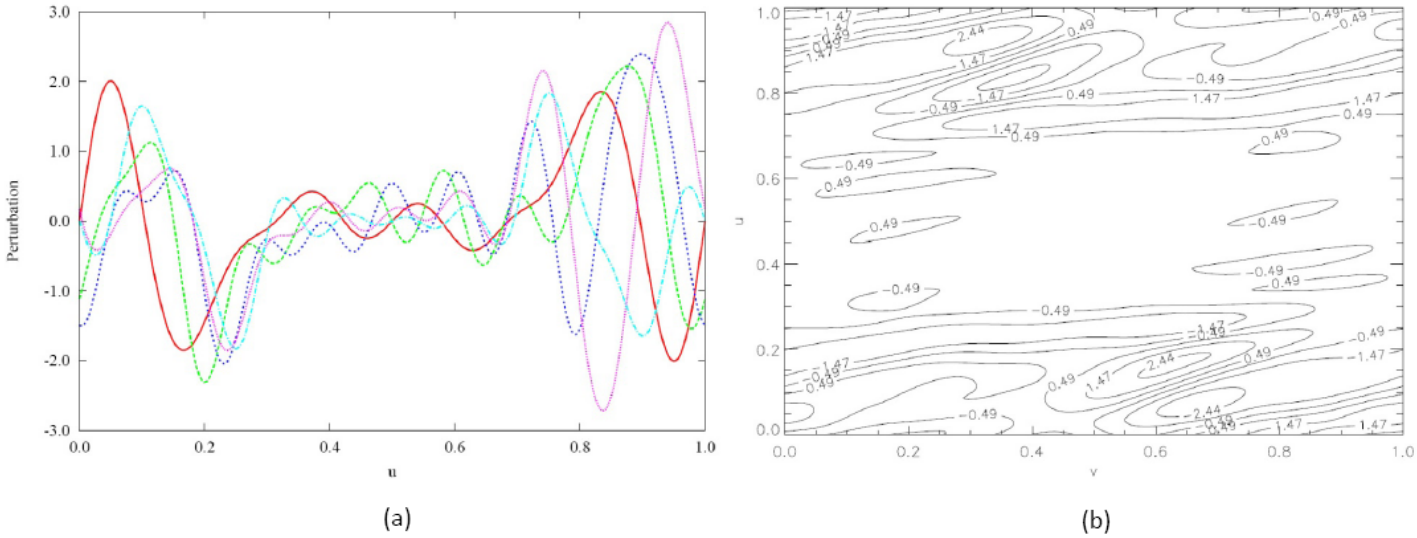

FIG. 8: (Color online) Perturbation distribution to which the N=1 kink stability is most sensitive in NCSX shown as function of the normalized poloidal angle u in five equally spaced toroidal angles over half a period (frame a) and in normalized toroidal and poloidal coordinates (frame b) on the LCMS. For (a) curves with color red (solid), green (dash), blue (short dash), magenta (dot) and light blue (dash-dot) correspond to $v = 0.0, 0.125, 0.25, 0.375$ and 0.5, respectively. For definitions of u and v, see figure 1.

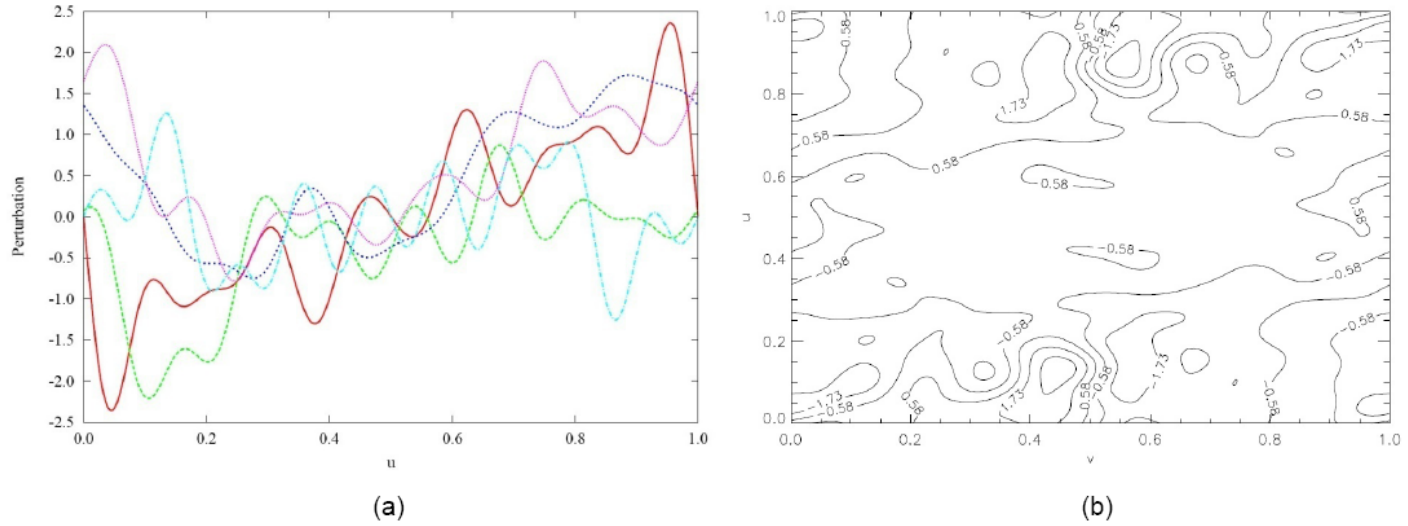

FIG. 9: (Color online) Perturbation distribution to which the effective helical ripple at $r/a \sim 0.7$ of NCSX is most sensitive shown as function of the normalized poidal angle u in five equally spaced toroidal angles over half a period (frame a) and in normalized toroidal and poloidal coordinates (frame b) on the LCMS. See caption of figure 8 for the color scheme for (a).

both the kink mode and the effective helical ripples the distributions show the sensitivity of plasma response to field errors mostly in outboard regions. For these distributions a perturbation of the external fields of 1% leads to a factor ~ 30 increase in the calculated eigenvalue or ~ 5.5 in the growth rate of the kink mode and a factor of ~ 1.5 increase in the effective helical ripple. For the kink stability, the most sensitive regions are those just off the outboard mid-plane near the crescent shaped section and those near the bottom tip of the cross section about two-third of the way toroidally between the crescent and the bullet shaped sections (the third cross section from the left in figure 1). For the effective ripple, the most sensitive regions are those also just off the mid-plane of the crescent shaped section as well as those near the outboard tip of the cross section close to the half-period bullet section. Of course, the stellarator symmetry applies to the other half-period. For NCSX the nominal magnetic strength is ~ 1.2 T so that perturbations in the range of tens of gauss would have significant effects

on the MHD stability of the configuration.

The most sensitive magnetic field perturbations for the kink stability shown in figure 8(b) change signs in a linear distance about $0.7a$, with a the average plasma minor radius. This indicates that corrections of the most sensitive magnetic perturbations affecting the kink stability are feasible for coils located at distances comparable to or smaller than the plasma minor radius a. For the effective ripple, the separation of the most sensitive regions with opposite signs is on the order of a. The control of magnetic perturbations for quasi-axisymmetry is less constrained.

IV. APPLICATION OF SENSITIVITY MATRIX TO COIL DESIGNS

The sensitivity matrix from BNPERT calculations can be incorporated into the design of primary coils to improve their characteristics. In coil designs, one attempts to minimize the normal fields on the boundary surface of the intended target plasma. The residues from the RMS minimization in the traditional procedure due to the limited number of Fourier modes to represent the current potential for the coils are usually on the order of a few percent, much larger than the magnitude of perturbations we have discussed. Nevertheless, coils designed with such processes are often found acceptable either because the physics properties of the resulting plasma are not degraded beyond the critical values or because further optimization of the coils may be carried out to recover the lost physics properties. In either case a neighboring equilibrium of the target plasma is found which has acceptable properties. The distribution of the residual errors is not known before the minimization and cannot be controlled in the process. The efficiency of this design process may be improved by taking advantage of the sensitivity response that is obtained through the process discussed in the previous sections. In particular, we find two useful applications: (a) use the response matrix to construct a basis for $\vec{b}\cdot\hat{n}$, (b) use the matrix elements to define an importance function (or weight) for $\vec{b}\cdot\hat{n}$.

The sensitivity matrix may be used to define a set of basis functions to represent normal magnetic fields on the plasma boundary. In general, in the design of stellarator coils, the objective is to find $[I]$ that minimizes the flux on the last closed magnetic surface in equation (9) except that now $[I]$ is constructed on a coil winding surface and the perturbation term on the right hand side is zero. As discussed in section II, equation (12), the response matrix may be decomposed into two orthonormal matrices $[V]$, $[U]$ and a matrix $[W]$ containing singular values. We construct a new basis $[h]$ defined by

$$[h] = [V]^T \cdot [f] \tag{13}$$

The magnetic flux expanded using this basis is a converging series with the ordering corresponding to the importance of the plasma response to various modes of perturbations. Using a subset of $[V]$, retaining only those with large singular values, we find coils that are less noisy but that the plasmas derived from them retain the important physics characteristics. In figure 10 we compare coil contours on a winding surface obtained from using a subset of $[V]$ to those derived from using the NESCOIL solution. NESCOIL [3] is a commonly used tool in designing stellarator coils but the algorithm it uses does not distinguish the relative importance of different modes of the normal magnetic fields. The subset used in this example included seventy-seven modes for the sensitivity response of the plasma aspect ratio, beta, rotational transform, effective helical ripples and stability to the kink and ballooning modes. The quality of quasi-axisymmetry and the characteristics of MHD stability of the new configuration remain essentially the same as the base configuration.

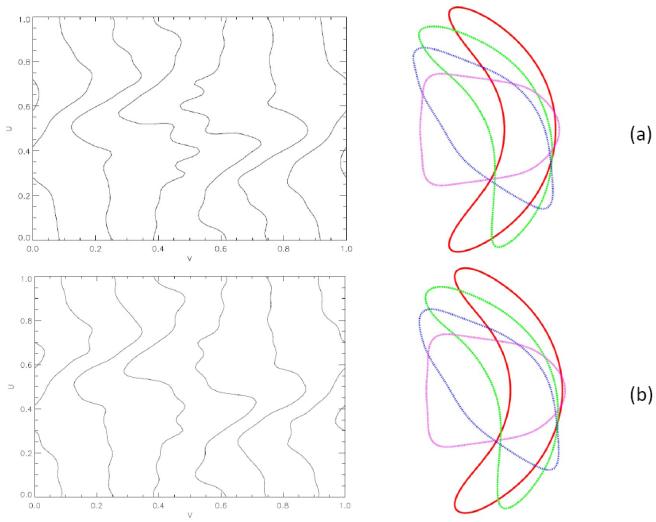

FIG. 10: (Color online) Comparison of contours of current potential on a winding surface uniformly displaced from the boundary of the NCSX baseline plasma by 0.14 units of the major radius. The contours are shown on the plane defined by the normalized toroidal (abscissa) and poloidal (ordinate) angles on the winding surface in one field period. The upper frame (a) is the solution obtained from the NESCOIL code with nine polodial modes and five toroidal modes for the current potential and the lower frame (b) is the solution using the basis derived from the sensitivity matrix with seventy-seven components. Shown on the right of each contour plot are the cross sections of the plasma in four equally spaced toroidal angles over half a period constructed by VMEC in the free-boundary mode using the current potential given on the left.

We note that if the size of $[I]$ is greater than the size of $[h]$ there is a so-called null space that would allow one to modify coil characteristics without changing the important normal magnetic fields on the plasma surface. In Ref. [16] the use of a resistance matrix has been proposed to minimize the power consumption and to bias

the current distribution on the coil winding surface.

The different types of response may also be combined into a total response function as discussed in section III. The column vector $[R]^T \cdot [\sigma]$ gives the relative importance on the quality of the plasma for each mode in $\vec{b} \cdot \hat{n}$ on the plasma surface. In codes commonly used for designing stellarator coils, such as NESCOIL or COILOPT [17], all modes of $\vec{b} \cdot \hat{n}$ are considered to be equally important. Using $[R]^T \cdot [\sigma]$ as a weight function to put more emphasis on minimizing the residue magnetic fields that have stronger adverse effects on the plasma properties of interest should produce better and more efficient coils. After all, the magnetic field distribution normal to the plasma boundary surface with a large perturbed response must be carefully controlled in designing coils.

Using the sensitivity function as an importance weighting for the normal field distribution on the plasma surface also leads to a larger condition number – the ratio of the largest to the smallest singular values when a matrix is decomposed with SVD – for the mutual inductance matrix $[M]$. For example, in NCSX the condition number with equal weighting of the perturbation response for the N=1 kink stability and the helical ripple is an order of magnitude larger than that without weighting. Since the current distributions on the winding surface associated with smaller singular values have lesser importance in contributing to the solution, we may select a subset of eigenvectors with the corresponding singular values exceeding only a certain threshold to define the coil geometry. Such a procedure reduces the complexity of coils and is useful for finding distant but buildable coils, although some of the important physics properties may be compromised in the process (because the distribution of the residue errors cannot be controlled before the process is complete, as discussed before). To recover the degraded or lost properties as a result of using the reduced set of singular values, we have developed a new procedure as follows. The solution for the current potential for each of the selected singular values is considered as a separate set of coils. The currents in these coils are then varied to find a plasma configuration satisfying all the targeted physics properties using tools such as STELLOPT [18]. The optimized currents are used to construct a set of re-scaled singular values and using them a new coil solution is obtained. The plasma derived from this new coil set should have identical properties as the one from the optimization of the currents for the singular coils. Mathematically, we introduce a set of scaling matrices $[S_k]$whose entries are all zero except for the k^{th} element that has a scaling s_k,

$$[I_k] = [V] \cdot [S_k] \cdot [W]^{-1} \cdot [U]^T \cdot [\vec{b} \cdot \hat{n}] \qquad (14)$$

and

$$[I] = \sum_k [I_k] \qquad (15)$$

where $[V]$ and $[U]$ are input and output matrices when $[M]$ is decomposed using SVD and $[W]$ is the diagonal matrix containing singular values. The scaling factors s_k are initially unity for the singular values retained in an analysis and zero for those discarded. The final values are obtained from the configuration re-optimization.

As an illustration, we show in figure 11 coil patterns for NCSX on a winding surface which is located at 0.21 units of the major radius away from the plasma LCMS. Solutions derived using both the method of NESCOIL and the method just described keeping about one-third of the eigenvectors are given. Also, results for both with and without optimization to rescale the singular values are shown in this figure. The importance function in this example was constructed with equal weighting for the kink stability and the effective helical ripples. Coils obtained from the SVD method are clearly less complex as the modes with lesser importance have been filtered out. Note that, for this case, the so-called coil aspect ratio, the ratio of the average plasma major radius to the distance separating the coil winding surface from the plasma LCMS, is about 4.8. It is almost as low as the plasma aspect ratio, which is 4.5. The low coil aspect ratio is considered to be one of the most important measures for being able to design compact, cost-competitive power reactors.

When the number of singular values retained is systematically varied and the current potential re-scaled to optimize the plasma performance, one often finds that there are many equilibria in the neighborhood of the target plasma that meet the most critically required criteria such as the MHD stability or quasi-symmetry for a configuration. The new method, thus, affords us an efficient means to identify an initial coil set that already has most of the desirable characteristics. Further optimization toward less complex, more buildable geometries becomes easier.

When a subset of the singular values is used in the mutual inductance matrix (without re-scaling), the solution for the current potential will only be approximate and the residue $\vec{b} \cdot \hat{n}$ on LCMS may be large. In the example given in figure 11(b) the average error over the surface is about 2% and the maximum error is nearly 16% of the local field strength. The equilibrium constructed based on this field distribution will not be MHD stable nor will it satisfy the quasi-symmetry criterion. When the configuration is re-optimized, the re-scaled current potential will yield another set of residues $\vec{b} \cdot \hat{n}$ on the original plasma surface. The magnitude of these residues has been observed to be as large as that before the re-optimization. Of course, the residues will vanish on the LCMS of the re-optimized plasma which has a different shape. The residues due to the re-scaled current potential on the original plasma surface give us an indication of which field error distributions are not important since the perturbed magnetic fields merely lead the plasma to a new neighboring equilibrium which recovers most of the properties of the reference plasma. We have analyzed the distributions of such residues and found that the general characteristics of the error field distribution look similar

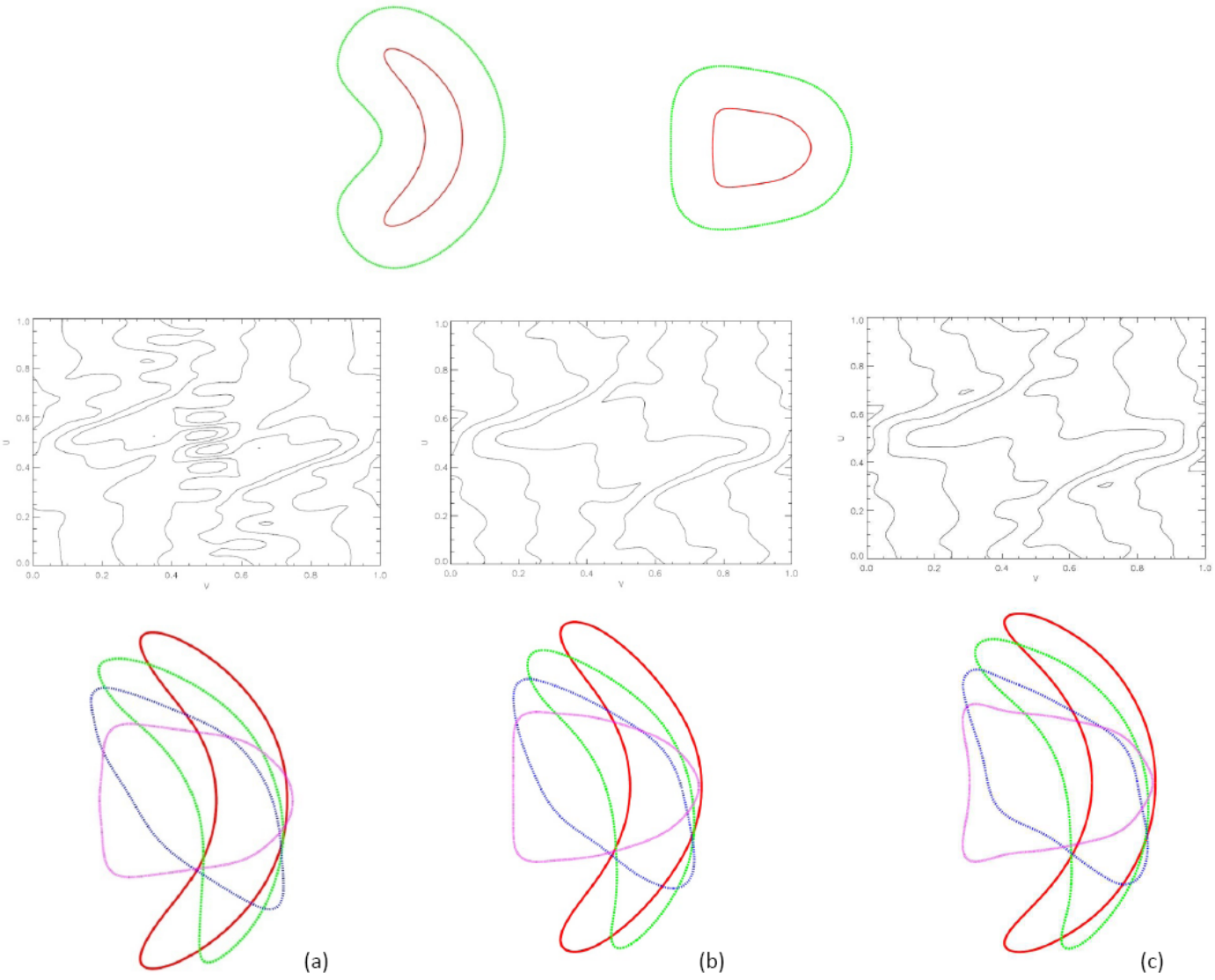

FIG. 11: (Color online) Coil contours on a current carry surface located at a distance of 0.21 units of the plasma major radius for NCSX. Shown on the top row are cross sections of the plasma boundary and the coil winding surface at the beginning of a period and at the half period. The current potential contours and the cross sections of the last closed magnetic surface of the constructed free boundary equilibrium are given in the next two rows in orders of (a) NESCOIL solution, (b) with 35 singular values retained in the mutual inductance, and (c) with 35 singular values retained in the mutual inductance whose values were rescaled based on the optimization of the plasma properties. Both the NESCOIL solution shown in (a) and the optimized solution with the reduced set of singular values shown in (c) recover the MHD stability and quasi-axisymmety properties of the baseline NCSX at 4%β while the solution shown in (b) does not. For the current potential, there were 9 poloidal mode and 5 toroidal modes used. The coil geometry is shown in a plane with the normalized toroidal angle v as the abscissa and the normalized poloidal angle u as the ordinate on the winding surface. For definitions of u and v, see figure 1.

before and after the re-optimization, as seen in figure 12. In both cases, the largest residues are at a region just off the in-board mid-plane near the half-period, bullet-shaped cross section. In section III we showed that both the kink stability and the effective ripple for NCSX are most sensitive to perturbations in the outboard regions. The large residue errors in the inboard regions for configurations in figures 11 (b) and (c) are apparently not that signifcant. This is the reason that it is possible to re-optimize the configuration from (b) to (c) shown in figure 11 to recover all the desirable properties. Indeed, a Fourier analysis for the residue distribution indicates that the largest contributing modes are $m = 1, n = 1$ and $m = 2, n = 1$, but neither is particularly important for perturbing the key physics properties of NCSX. This example clearly demonstrates the importance of understanding the plasma sensitivity to the distributions of external magnetic field perturbations.

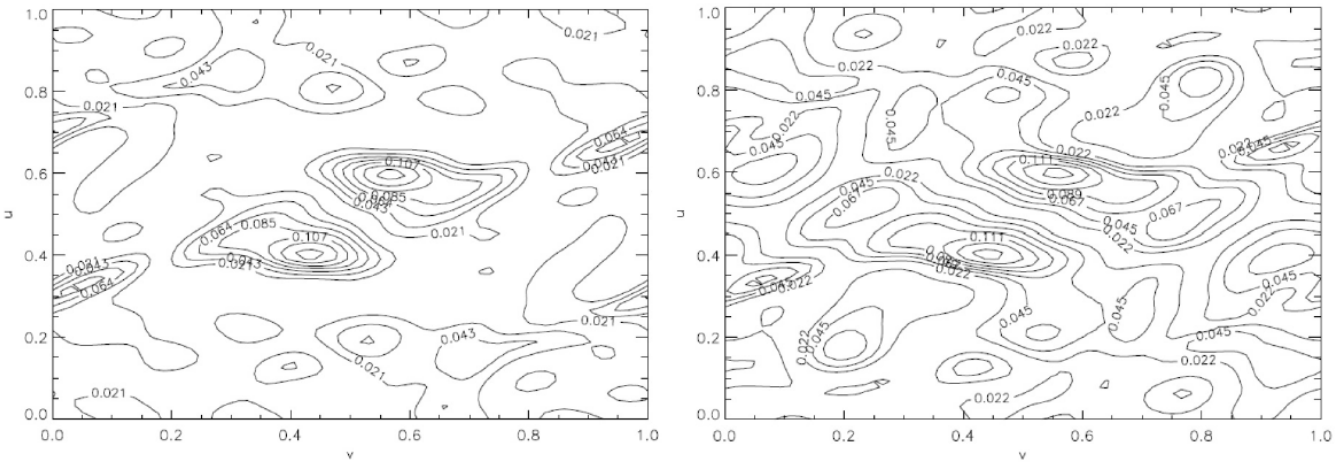

FIG. 12: (Color online) Contours of residue magnetic fields normal to the LCMS of NCSX for cases b and c shown in figure 11, case b: left frame; case c: right frame. The residue fields are normalized to the local field strengths and shown in a coordinate system on the LCMS defined by the normalized poloidal angle u and toroidal angle v. For definitions of u and v, see figure 1.

Finally, the sensitivity matrix can be used directly in the design of trim coils to correct field errors of small magnitudes. Let $[T]$ be the matrix relating the change in the plasma properties to the change in the trim coil current. The magnitude of currents required to null out the known error field is simply

$$[I_t] = -[T]^{-1} \cdot [R] \cdot [\delta\vec{b} \cdot \hat{n} / \mid \vec{b} \mid] \tag{16}$$

V. SUMMARY AND CONCLUSIONS

A numerical method has been developed that applies small magnetic perturbations directly to the plasma boundary to evaluate the plasma response to the perturbations. The derived plasma response matrix gives the sensitivity of an equilibrium to the external perturbations and singles out error field distributions that need to be carefully controlled. Using the information contained in the response matrix one can design coils more effectively so that more robust coils may be realized at a distance farther from the plasma. In particular, by optimizing a selected set of singular values in the mutual inductance matrix equilibria in the neighborhood of the target plasma having similarly desirable physics properties can be identified that may be produced by coils with less complexity. By using only a subset of the current potential to optimize plasma properties, one is left with additional rooms that can be used to further improve coil characteristics.

The present work may be extended to study the amplification of the *total* magnetic field harmonics at the plasma boundary, in addition to looking at the overall physical response such as the MHD stability or quasi-axisymmetry. The total $\vec{b} \cdot \hat{n}$ at the plasma boundary provides us important information useful for the plasma control. While we have discussed the distributions of the magnetic perturbations that the kink stability and effective ripples are most sensitive to for NCSX, it is possible to construct distributions that are orthogonal to the most sensitive ones to understand how fast the series converges and how many important distributions need to be controlled. Using SVD to filter out certain harmonic content in the current potential has been shown to be able to reduce the complexity of coils. It will be useful to extend the study to find out how the re-calibrated singular values relate to the distance separating the current carrying surface from the plasma boundary and how the characteristics of the distant coils change. Finally, if the number of parameters used to specify the geometry of coils is greater than the number of parameters required to described the desirable phyiscs characteristics of a plasma, a null space exists. Finding the best use of the null space to simplify coil topology remains an interesting and challenging subject.

Acknowledgements

This work was supported by U. S. Department of Energy through the grant ER54333 to Columbia University and the contract DE-AC02-09CH11466 to the Princeton Plasma Physics Laboratory. The authors are indebted to W. A. Cooper, S. P. Hirshman, W. Kernbichler, J. Nuhrenberg, P, Merkel, R. Sanchez and other co-authors of TERPSICHORE, VMEC, NEO, JMC, NESCOIL and COBRA for making the computer codes available to us in this work. The authors would also like to acknowledge useful discussions with N. Pomphrey.

[1] F. Bauer, O. Betancourt and P. Garabedian; *Magneto-hydrodynamic Equilibrium and Stability of Stellarators*, Springer-Verlag, New York (1984).

[2] A. Boozer, Physics of Plasmas, **7**, 3378 (2000).

[3] P. Merkel, Nuclear Fusion, **27**, 867 (1987).

[4] N. Pomphrey, L. Berry, A. Boozer, A. Brooks, R. E. Hatcher, S. P. Hirshman, L. P. Ku, W. H. Miner, H. E. Mynick, W. Reiersen, D. J. Strickler and P. M. Valanju, Nuclear Fusion, **41**, 339 (2001)

[5] R. Schmidtt, Fusion Science and Technology, **57**, 152 (2010).

[6] L. P. Ku, P. R. Garabedian, J. Lyon, A. Turnbull, A. Grossman, T. K. Mau, M. Zarnstorff and the ARIES Team, Fusion Science and Technology, **54**, 673 (2008).

[7] A. H. Boozer, Physics of Plasmas, **6**, 831 (1999).

[8] S. P. Hirshman, W. I. van Rij and P. Merkel, Comput. Phys. Commun. **43**, 143 (1986).

[9] A. Reiman and H. Greenside, Comput. Phys. Commun. **43** 157 (1986).

[10] D. Anderson, W. A. Cooper, R. Gruber, S. Merazzi and U. Schwenn, Scient. Comput. Supercomput. II, 159 (1990).

[11] R. Sanchez, S. P. Hirshman, J. C. Whitson and A. S. Ware, J. Comput. Phys., **161**, 589 (2000).

[12] J. Nuhrenberg and R. Zille, Proc. of the IAEA Technical Committee Meeting on Plasma Confinement and Heating in Stellarators, Schloss Ringberg, Germany, September 24-28 (1984).

[13] V. V. Nemov, S. V. Kasilov, W. Kernbichler and M. F. Heyn, Phys. Plasma, **6**, 4622 (1999).

[14] A. Boozer, Phys. Fluids **24**, 1999 (1981).

[15] M. C. Zarnstorff, L. A. Berry, A. Brooks, E. Fredrickson, G. Y. Fu, S. Hirshman, S. Hudson, L. P. Ku, E. Lazarus, D. Mikkelsen, D. Monticello, G. H. Neilson, N. Pomphrey, A. Reiman, D. Spong, D. Strickler, A. Boozer, W. A. Cooper, R. Goldston, R. Hatcher, M. Isaev, C. Kessel, J. Lewandowski, J. F. Lyon, P. Merkel, H. Mynick, B. E. Nelson, C. Nuehrenberg, M. Redi, W. Reiersen, P. Rutherford, R. Sanchez, J. Schmidt and R. B. White, Plasma Phys. Control. Fusion **43**, A237 (2001).

[16] A. Boozer, Physics of Plasmas, **7**, 629 (2000).

[17] D. J. Strickler, L. A. Berry and S. P. Hirshman, Fusion Science and Technology, **41**, 107 (2002).

[18] D. J. Strickler, L. A. Berry, S. P. Hirshman, J. F. Lyon, D. A. Spong, D. E. Williamson, M. C. Zarnstorff, L. P. Ku, A. Brooks, S. R. Hudson, D. A. Monticello, G. H. Neilson, N. Pomphrey, A. H. Reiman, A. S. Ware, Proc. 19th Fusion Energy Conf., Lyon, France. FT/P2-06, October (2002).

The Princeton Plasma Physics Laboratory is operated
by Princeton University under contract
with the U.S. Department of Energy.

Information Services
Princeton Plasma Physics Laboratory
P.O. Box 451
Princeton, NJ 08543

Phone: 609-243-2245
Fax: 609-243-2751
e-mail: pppl_info@pppl.gov
Internet Address: http://www.pppl.gov